

~~CONFIDENTIAL~~

Copy 214  
RM L55A19

NACA RM L55A19



NACA

# RESEARCH MEMORANDUM

AERODYNAMIC CHARACTERISTICS OF A 60° DELTA WING HAVING A  
HALF-DELTA TIP CONTROL AT A MACH NUMBER OF 4.04

By Edward F. Ulmann and Fred M. Smith

Langley Aeronautical Laboratory  
Langley Field, Va.

Classification cancelled (or changed to Unclassified)

by Author NASA Tech Pub Announcement #33  
(OFFICER AUTHORIZED TO CHANGE)

By 24 Nov 60

NK

GRADE OR OFFICE (AUTHOR TO CHANGE)

13 Feb 61 DATE CLASSIFIED DOCUMENT

This material contains information affecting the National Defense of the United States within the meaning of the espionage laws, Title 18, U.S.C., Secs. 793 and 794, the transmission or revelation of which in any manner to an unauthorized person is prohibited by law.

NATIONAL ADVISORY COMMITTEE  
FOR AERONAUTICS

WASHINGTON

April 25, 1955

~~CONFIDENTIAL~~



0144195

## NATIONAL ADVISORY COMMITTEE FOR AERONAUTICS

## RESEARCH MEMORANDUM

AERODYNAMIC CHARACTERISTICS OF A  $60^\circ$  DELTA WING HAVING A  
HALF-DELTA TIP CONTROL AT A MACH NUMBER OF 4.04

By Edward F. Ulmann and Fred M. Smith

## SUMMARY

An investigation has been conducted in the Langley 9- by 9-inch Mach number 4 blowdown jet to determine the aerodynamic characteristics of a  $60^\circ$  delta wing with a half-delta tip control at a Mach number of 4.04 and a Reynolds number of  $5.8 \times 10^6$ , based on the wing mean aerodynamic chord. The results of the investigation were compared with the predictions of linear theory and the two-dimensional shock-expansion theory. The two-dimensional shock-expansion theory gave improved predictions of the lift and roll characteristics, but gave less accurate predictions of the hinge-moment parameters. The hinge-line location of these tests (59.6-percent control root chord) resulted in stable variations of the hinge-moment coefficient with control deflection and angle of attack, except for an angle of attack of  $12^\circ$  for control deflections from  $0^\circ$  to  $-6^\circ$ . A comparison was made of the rolling effectiveness of the test configuration with that of a rectangular wing having the same span and a 30-percent-chord trailing-edge flap. The comparison showed that the increased effectiveness of the tip control over the full-span trailing-edge control, which has been observed at lower supersonic Mach numbers, is also present at a Mach number of 4.

## INTRODUCTION

Numerous tests of tip controls on delta wings at transonic and low supersonic speeds have shown that such configurations provide satisfactory rolling-moment effectiveness, and that the hinge moments can be controlled by proper location of the hinge line (ref. 1).

The purpose of the present tests is to determine the characteristics of such a configuration at a Mach number of 4.04 and a Reynolds number of  $5.8 \times 10^6$ , based on the wing mean aerodynamic chord. The wing and control plan form, location of the hinge line, and ratio of the control to the wing area are the same as those of one of the wings tested at a

~~CONFIDENTIAL~~~~CONFIDENTIAL~~

Mach number of 1.61 (ref. 1). The airfoil section is different, however, in that it has a sharp leading edge instead of the rounded leading edge tested at a Mach number of 1.61. The sharp leading-edge section was considered to be of more interest since in reference 2 it was shown that at a Mach number of 4.04 the wing with this section had 30 percent lower minimum drag and 22 percent higher maximum lift-drag ratio than the same wing with the rounded leading-edge section. The sharp leading-edge wing and control were also tested at a Mach number of 6.9 (ref. 3), but only the control hinge-moment characteristics were obtained.

Lift, drag, pitching-moment, rolling-moment, and hinge-moment coefficients are presented for the test configuration through an angle-of-attack range from  $0^\circ$  to  $12^\circ$  and a control-deflection range from approximately  $-16^\circ$  to  $14^\circ$ .

#### SYMBOLS

M	free-stream Mach number
q	free-stream dynamic pressure
c	wing root chord
$\bar{c}$	wing mean aerodynamic chord, $\frac{2}{3} c$
b	wing span, twice semispan
$c_f$	control root chord
$\bar{c}_f$	control mean aerodynamic chord, $\frac{2}{3} c_f$
$b_f$	control span
S	area of semispan wing
$S_f$	area of control
$\alpha$	wing angle of attack
$\delta$	control-deflection angle relative to chord of wing, positive with trailing edge deflected downward
R	Reynolds number based on wing mean aerodynamic chord

~~CONFIDENTIAL~~

N	normal force of semispan wing and control
L	lift of semispan wing and control
D	drag of semispan wing and control
M'	pitching moment about $0.5\bar{c}$
H	control hinge moment about hinge line, positive when tending to deflect trailing edge downward
L'	wing rolling moment about wing root, positive when tending to roll right wing downward
$\Delta L'$	rolling moment due to control deflection
$C_N$	normal-force coefficient, $N/qS$
$C_L$	lift coefficient, $L/qS$
$C_D$	drag coefficient, $D/qS$
$\Delta C_D$	incremental drag due to control deflection, $(C_{D\delta} - C_{D\delta=0})_{\alpha=\text{constant}}$
$C_m$	pitching-moment coefficient, $M'/q\bar{c}S$
$C_h$	control hinge-moment coefficient, $H/q\bar{c}_f S_f$
$C_{l_{\text{gross}}}$	gross rolling-moment coefficient, $L'/2qSb$
$C_l$	rolling-moment coefficient due to control deflection, $C_{l_{\text{gross}}} - (C_{l_{\text{gross}}})_{\delta=0}$
L/D	ratio of wing lift to wing drag
$pb/2V$	wing-tip helix angle
p	rolling angular velocity
V	free-stream airspeed
$C_{l_p}$	damping-in-roll coefficient, $\partial C_l / \partial \frac{pb}{2V}$

$C_{L_\alpha}$	lift-curve slope, $\partial C_L / \partial \alpha$
$C_{L_\delta}$	rate of change of lift coefficient with control deflection, $\partial C_L / \partial \delta$
$C_{h_\alpha}$	rate of change of control hinge-moment coefficient with angle of attack, $\partial C_h / \partial \alpha$
$C_{h_\delta}$	rate of change of control hinge-moment coefficient with control deflection, $\partial C_h / \partial \delta$
$C_{l_\delta}$	rate of change of rolling-moment coefficient with control deflection, $\partial C_l / \partial \delta$

#### APPARATUS AND TESTS

The tests were conducted in the Langley 9- by 9-inch Mach number 4 blowdown jet. A description of the jet along with a test-section flow calibration is presented in reference 4. The settling-chamber pressure, which was controlled by a pressure-regulating valve and was continuously recorded during each run, was approximately 185 lb/sq in. abs. The settling-chamber temperature was also continuously recorded during each run. An external side-wall-mounted strain-gage balance was used to measure the normal force, chord force, pitching moment, and rolling moment of the model. A strain-gage beam mounted on the wing support (fig. 1) was used to measure the control hinge moment. Schematic diagrams showing the wing mounting and test-section orientation are shown in figures 1 and 2.

The Reynolds number for the tests was  $5.8 \times 10^6$ , based on the wing mean aerodynamic chord. Because of the balance limitations, the angle-of-attack range was held to  $0^\circ$  to  $12^\circ$  and the control-deflection range was approximately  $-16^\circ$  to  $14^\circ$ . The tests were made at humidities below  $5 \times 10^{-6}$  pounds of water vapor per pound of dry air; such humidities are believed to be low enough to eliminate water-condensation effects. The test-section static temperature and pressure did not reach the point where liquefaction of air would occur.

~~CONFIDENTIAL~~

## MODEL

The model (fig. 3) consisted of a steel semispan wing of delta plan form with a  $60^\circ$  sweptback leading edge, an aspect ratio of 2.31, and a symmetrical modified hexagonal section 3 percent thick at the root. The section consisted of a wedge-shaped leading edge, a parallel-sided mid-section, and a half-blunt wedge-shaped trailing edge. The wing was of constant thickness out to the 56.3-percent-semispan station. The area beyond the 56.3-percent-semispan station formed the half-delta control surface. The control had an area equal to 19 percent of the wing area. A gap of 0.002 to 0.005 inch was provided for clearance between control surface and wing. The control-surface hinge line was located at 59.6 percent of the control root chord.

## PRECISION OF DATA

The uncertainties involved in measuring the angles, forces, and moments, and in determining the aerodynamic coefficients have been evaluated. The probable uncertainties are listed as follows:

$\alpha$ , deg . . . . .	$\pm 0.1$
$\delta$ , deg . . . . .	$\pm 0.1$
$C_L$ . . . . .	$\pm 0.005$
$C_D$ . . . . .	$\pm 0.001$
$C_m$ . . . . .	$\pm 0.001$
$C_z$ . . . . .	$\pm 0.003$
$C_h$ . . . . .	$\pm 0.003$

## THEORETICAL METHODS

The lift, rolling-moment, and hinge-moment parameters of the wing and control were estimated by linear theory (refs. 5 and 6) and by the two-dimensional shock-expansion theory. The latter method, which is based on considerations of the similarity of the flows over delta wings with and without thickness, has been shown to give good predictions of the lift-curve slopes of the wing used in this investigation and of other sharp leading-edge-section delta wings with attached leading-edge shocks (ref. 7). The predictions of the method have also been compared with experimental hinge-moment slopes obtained at a Mach number of 6.9 on the control used in this investigation and on one other tip control (ref. 3). It was found that, at a Mach number of 6.9, the shock-expansion theory generally gave better predictions than the linear theory.

~~CONFIDENTIAL~~

The theoretical drag coefficient of the wing at zero lift was computed in two parts: pressure drag and skin-friction drag. The pressure drag was obtained by integrating the chordwise components of the surface pressure computed by the two-dimensional shock-expansion theory and by including in the integration an experimental base-pressure coefficient from reference 8. This method follows from the analysis of reference 7, which showed that the pressure-drag coefficients of thin double-wedge-section delta wings with attached leading-edge shocks were closely approximated by the shock-expansion two-dimensional drag of the wing sections.

The skin-friction drag was estimated by using Van Driest's theoretical values of laminar and turbulent skin-friction coefficients (refs. 9 and 10) and a transition point obtained from boundary-layer visualization tests of the wing.

The experimental drag coefficients are compared with theoretical drag coefficients computed on the assumptions that there is no variation of chord force with angle of attack and that the drag due to lift is equal to the streamwise component of theoretical shock-expansion normal force. These assumptions have been justified by tests of low-aspect-ratio wings at supersonic speeds (refs. 7 and 11).

The chordwise and spanwise centers of pressure of the wing-control combination near  $\alpha = 0^\circ$  and  $\delta = 0^\circ$  were obtained by linear theory and by the two-dimensional shock-expansion theory. As a first approximation of the center-of-pressure locations at higher angles of attack and control deflections, the gap effects between the wing and control were considered negligible, and two-dimensional loading proportional to the total deflection ( $\alpha + \delta$ ) was assumed to apply independently to the wing and the control.

## RESULTS AND DISCUSSION

The basic aerodynamic data for the test configuration are presented as functions of lift coefficient, control deflection, and angle of attack in figures 4 to 7. Figures 8 and 9 present a comparison of the rolling effectiveness of the control tested with the rolling effectiveness of a full-span 30-percent-chord trailing-edge flap on an aspect-ratio-1.33 rectangular-plan-form wing (ref. 12).

### Effects of Changes in Angle of Attack and Control Deflection

Changes in angle of attack or control deflection produce approximately linear changes in lift coefficient, pitching-moment coefficient, and rolling-moment coefficient (figs. 4, 5, and 6). The drag curves have the usual parabolic shape with the minimum drag and the maximum lift-drag ratio occurring at a control deflection of  $0^\circ$ , as might be expected (figs. 4(a) and 4(b)). Variations of the hinge-moment coefficient with changes in angle of attack or control deflection are approximately linear until the angle of attack exceeds about  $4^\circ$  (fig. 5). Tests of configurations having the same wing and control plan form and ratio of the control to the wing area at Mach numbers of 6.9 and 1.61 (refs. 3 and 13) show approximately the same trends. It should be noted that the wing tested at a Mach number of 1.61 had a slightly different airfoil section. The nonlinearities in hinge moment are caused by shifts of the center of pressure of the control normal force, since the variations of wing lift with angle of attack and control deflection are approximately linear.

The data show a stable variation of hinge moment with control deflection, except at  $12^\circ$  angle of attack between control deflections of  $-6^\circ$  and  $0^\circ$ . The hinge-moment variation with angle of attack for constant control deflections is stable throughout the tests. The tests at a Mach number of 1.61 (ref. 13) show approximately the same regions of stable and unstable hinge-moment variation as the present tests. Reference 3, which reports tests on this configuration at a Mach number of 6.9, shows stable hinge-moment variations throughout the range of the tests, but does not present hinge-moment variation with control deflection for angles of attack greater than  $8^\circ$ .

### Comparison of Experimental Results With Theoretical Predictions

The wing-lift and rolling-moment slope parameters, as predicted by linear theory, were low in every case, as shown in table I. The shock-expansion theory, however, gave improved predictions of wing lift due to angle of attack, lift due to control deflection, and rolling moment due to control deflection. The differences between experimental results and theoretical predictions were reduced from 13 percent to 5 percent for  $C_{L_\alpha}$ , from 27 percent to 15 percent for  $C_{L_\delta}$ , and from 11 percent to 3 percent for  $C_{l_\delta}$  by the use of the shock-expansion theory instead of linear theory.

The minimum drag of the wing was fairly well predicted by theory, as shown in figure 4(a). The drag due to lift at zero control deflection was well predicted by the simple resolution of the normal and chord

~~CONFIDENTIAL~~



forces, also shown in figure 4(a). The fact that the drag due to lift at constant angle of attack was somewhat underestimated at the higher control deflections (see also fig. 6(b)) indicated that considerable drag is induced by the flow through the gap between the wing and control. Flow separation over the upper surface of the control, although likely to be present at high total control deflections, would not increase but would actually reduce the drag. The predicted maximum lift-drag ratio (fig. 4(b)) for zero control deflection was 11 percent higher than the experimental value, which is not surprising since the predicted drag was lower than experimental drag.

Near  $0^\circ$  angle of attack and control deflection, linear theory predicts the chordwise center-of-pressure location to be 66.7 percent of the root chord from the wing apex. The experimental chordwise center-of-pressure location  $C_m/C_N$  was found to be approximately 66 percent of wing root chord from the apex. The chordwise center-of-pressure location was predicted more accurately by linear theory than by the shock-expansion theory, which gave a value of 64.3 percent of root chord. Also near  $0^\circ$  angle of attack and control deflection, the linear theory predicts the spanwise center-of-pressure location of the wing to be 35.4 percent wing semispan from the root chord, and the shock-expansion theory gives a predicted value of 34.3 percent. The experimental spanwise center-of-pressure location was found to be approximately 38 percent wing semispan from the root chord. Predictions of center-of-pressure locations at angles of attack and control deflections other than  $0^\circ$  were usually within 5 percent of the wing root chord or wing semispan of the experimental results, as shown in figure 7. An exception to this is the  $\alpha = 0^\circ$  curve which shows large disagreement between the experimental and theoretical values of spanwise center of pressure at the low control deflections. Except for the low forces involved, there is no apparent reason for this disagreement.

The control hinge-moment parameters  $C_{h_\alpha}$  and  $C_{h_\delta}$  are somewhat more accurately predicted by linear theory than by shock-expansion two-dimensional theory, especially in the case of  $C_{h_\alpha}$  (table I). The reasons for this cannot be determined from the present data since measurements of the control normal force were not made, and, therefore, the center of pressure of the control normal force could not be obtained. It is realized, of course, that the use of the two-dimensional shock-expansion theory to predict  $C_{h_\alpha}$  and  $C_{h_\delta}$  for this configuration at a Mach number of 4.0 is more likely to give poor predictions than at a Mach number of 6.9, where it gave good predictions (ref. 3), because of the larger area of three-dimensional flow over the control at the lower Mach number.

CONFIDENTIAL

## Comparison of the Rolling Effectiveness of the Test Configuration

## With That of a Rectangular Wing Having a Full-Span

## Trailing-Edge Flap Control

The rolling effectiveness  $pb/2V\delta$  for the test configuration and the configuration of reference 12, which have the same wing span, was computed by using the experimental value of  $C_{l\delta}$  and theoretical values of the damping-in-roll coefficient  $C_{lp}$  from reference 14 and is given in the following table:

Configuration		$C_{l\delta}$ (experimental)	$C_{lp}$ (theoretical, ref. 14)	$\frac{pb/2V}{\delta}$
Wing plan form	Type of control			
Delta	Half-delta tip	-0.00066	-0.085	0.0083
Rectangular	30-percent-chord trailing-edge flap	-.00044	-.1245	.0035

Although the ratio of control to wing area for the delta configuration is only 63 percent of that of the rectangular configuration with trailing-edge flap, the delta configuration produces 50 percent more rolling moment and has about 125 percent greater rolling effectiveness. Two reasons for the improved effectiveness of the delta wing and control over the rectangular wing and flap are that the tip control area is more favorably located, and the delta wing has much lower damping in roll. This improved effectiveness has been demonstrated by many investigations at lower supersonic Mach numbers.

For the same wing-tip helix angle  $pb/2V$ , the full-span rectangular flap produces approximately 150 percent as much incremental drag as the tip control at all angles of attack (fig. 8).

A further comparison of the test wing and the wing of reference 12 is shown in figure 9. The parameter plotted is the ratio of rolling-moment slope to hinge-moment slope for each wing. A large number indicates good rolling characteristics for a given hinge moment, whereas a small number indicates poor rolling characteristics. It can be seen

~~CONFIDENTIAL~~

that the value for the test wing is from 4 to 7 times greater than the value for the wing of reference 12.

#### CONCLUDING REMARKS

An investigation has been conducted in the Langley 9- by 9-inch Mach number 4 blowdown jet to determine the aerodynamic characteristics of a  $60^\circ$  delta wing with a half-delta tip control at a Mach number of 4.04 and a Reynolds number of  $5.8 \times 10^6$ , based on the wing mean aerodynamic chord. The results of the investigation were compared with the predictions of linear theory and the two-dimensional shock-expansion theory. The two-dimensional shock-expansion theory gave improved predictions of the lift and roll characteristics, but gave less accurate predictions of the hinge-moment parameters. The hinge-line location of these tests (59.6-percent control root chord) resulted in stable variations of the hinge-moment coefficient with control deflection and angle of attack, except for an angle of attack of  $12^\circ$  for control deflections from  $0^\circ$  to  $-6^\circ$ . A comparison was made of the rolling effectiveness of the test configuration with that of a rectangular wing having the same span and a 30-percent-chord trailing-edge flap. The comparison showed that the increased effectiveness of the tip control over the full-span trailing-edge control, which has been observed at lower supersonic Mach numbers, is also present at a Mach number of 4.

Langley Aeronautical Laboratory,  
National Advisory Committee for Aeronautics,  
Langley Field, Va., January 11, 1955.

~~CONFIDENTIAL~~

## REFERENCES

1. Lord, Douglas R., and Czarnecki, K. R.: Aerodynamic Characteristics of Several Tip Controls on a  $60^\circ$  Delta Wing at a Mach Number of 1.61. NACA RM L54E25, 1954.
2. Dunning, Robert W., and Smith, Fred M.: Aerodynamic Characteristics of Two Delta Wings and Two Trapezoidal Wings at Mach Number 4.04. NACA RM L53D30a, 1953.
3. Fetterman, David E., and Ridyard, Herbert W.: The Effect of a Change in Airfoil Section on the Hinge-moment Characteristics of a Half-Delta Tip Control With a  $60^\circ$  Sweep Angle at a Mach Number of 6.9. NACA RM L54H16a, 1954.
4. Ulmann, Edward F., and Lord, Douglas R.: An Investigation of Flow Characteristics at Mach Number 4.04 Over 6- and 9-Percent-Thick Symmetrical Circular-Arc Airfoils Having 30-Percent-Chord Trailing-Edge Flaps. NACA RM L51D30, 1951.
5. Tucker, Warren A., and Nelson, Robert L.: Theoretical Characteristics in Supersonic Flow of Two Types of Control Surfaces on Triangular Wings. NACA Rep. 939, 1949. (Supersedes NACA TN's 1600 & 1601 by Tucker and TN 1660 by Tucker & Nelson.)
6. Kainer, Julian H., and King, Mary Dowd: The Theoretical Characteristics of Triangular-Tip Control Surfaces at Supersonic Speeds. Mach Lines Behind Trailing Edges. NACA TN 2715, 1952.
7. Ulmann, Edward F., and Bertram, Mitchel H.: Aerodynamic Characteristics of Low-Aspect-Ratio Wings at High Supersonic Mach Numbers. NACA RM L53I23, 1953.
8. Klunker, E. B., and Harder, Keith C.: Comparison of Supersonic Minimum-Drag Airfoils Determined by Linear and Nonlinear Theory. NACA TN 2623, 1952.
9. Van Driest, E. R.: Investigation of Laminar Boundary Layer in Compressible Fluids Using the Crocco Method. NACA TN 2597, 1952.
10. Van Driest, E. R.: The Turbulent Boundary Layer for Compressible Fluids on a Flat Plate With Heat Transfer. Rep. No. AL-997, North American Aviation, Inc., Jan. 27, 1950.
11. Hall, Charles F.: Lift, Drag, and Pitching Moment of Low-Aspect-Ratio Wings at Subsonic and Supersonic Speeds. NACA RM A53A30, 1953.

~~CONFIDENTIAL~~

12. Dunning, Robert W., and Ulmann, Edward F.: Aerodynamic Characteristics at Mach Number 4.04 of a Rectangular Wing of Aspect Ratio 1.33 Having a 6-Percent-Thick Circular-Arc Profile and a 30-Percent-Chord Full-Span Trailing-Edge Flap. NACA RM L53D03, 1953.
13. Czarnecki, K. R., and Lord, Douglas R.: Hinge-Moment Characteristics for Several Tip Controls on a 60° Sweptback Delta Wing at Mach Number 1.61. NACA RM L53K28, 1953.
14. Harmon, Sydney M., and Jeffreys, Isabella: Theoretical Lift and Damping in Roll of Thin Wings With Arbitrary Sweep and Taper at Supersonic Speeds - Supersonic Leading and Trailing Edges. NACA TN 2114, 1950.

TABLE I.- WING AND CONTROL PARAMETERS

Parameter	Linear theory	Shock-expansion theory	Experimental value
$C_{L\alpha}$	0.0178	0.0194	0.0205
$C_{L\delta}$	.0033	.0038	.0045
$C_{L\dot{\delta}}$	-.00059	-.00068	-.00066
$C_{h\delta}$	-.0029	-.0016	-.0023
$C_{h\alpha}$	-.00354	-.0016	-.0037

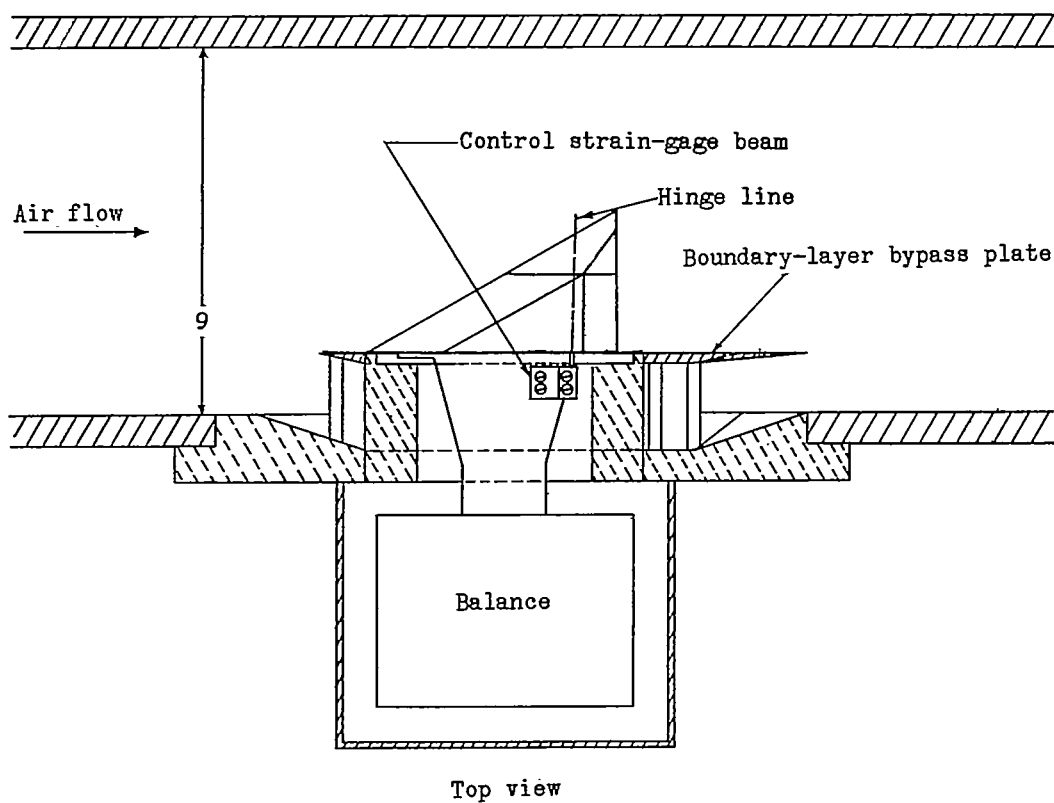
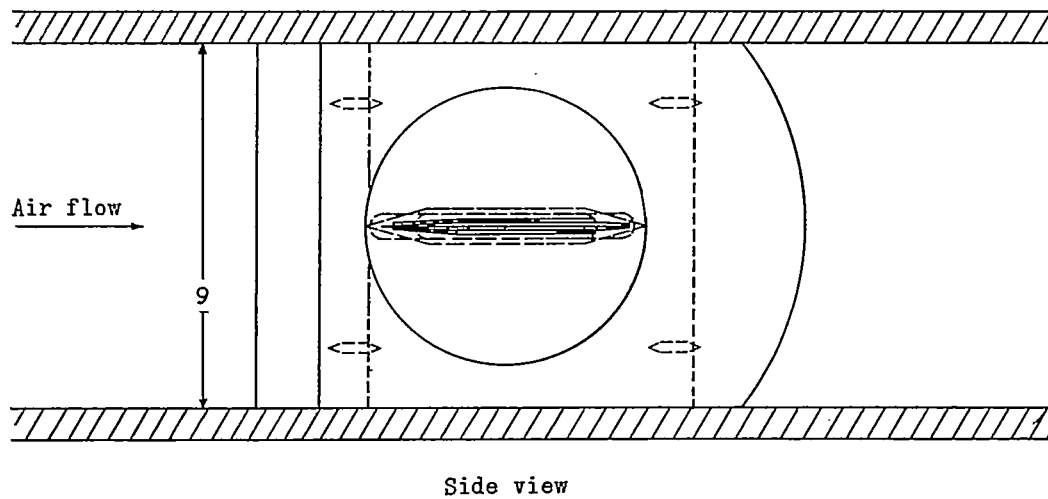


Figure 1.- Schematic diagram of test section of Langley 9- by 9-inch Mach number 4 blowdown jet and balance arrangement. All dimensions are in inches.

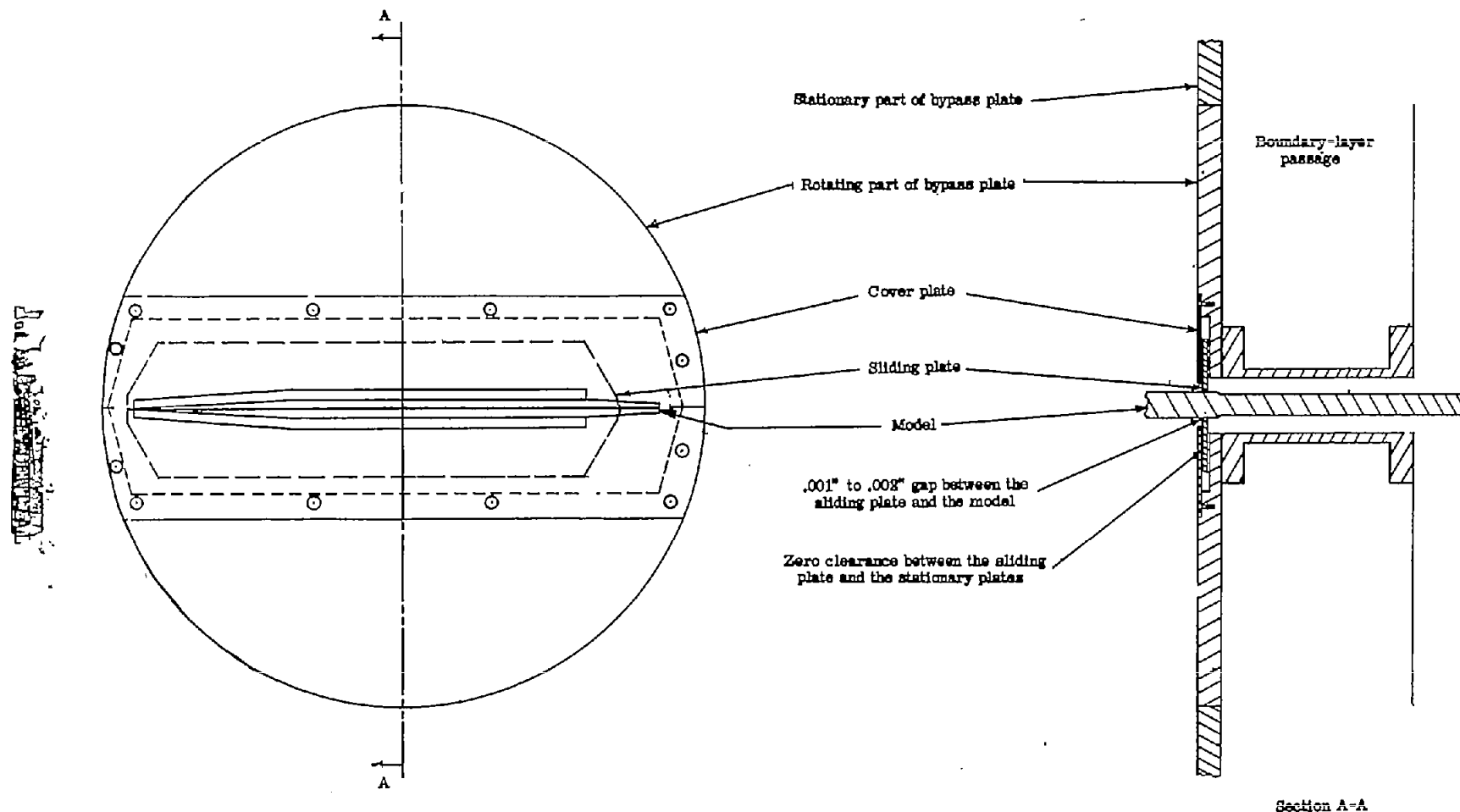


Figure 2.- Sliding-plate gap-sealing mechanism.



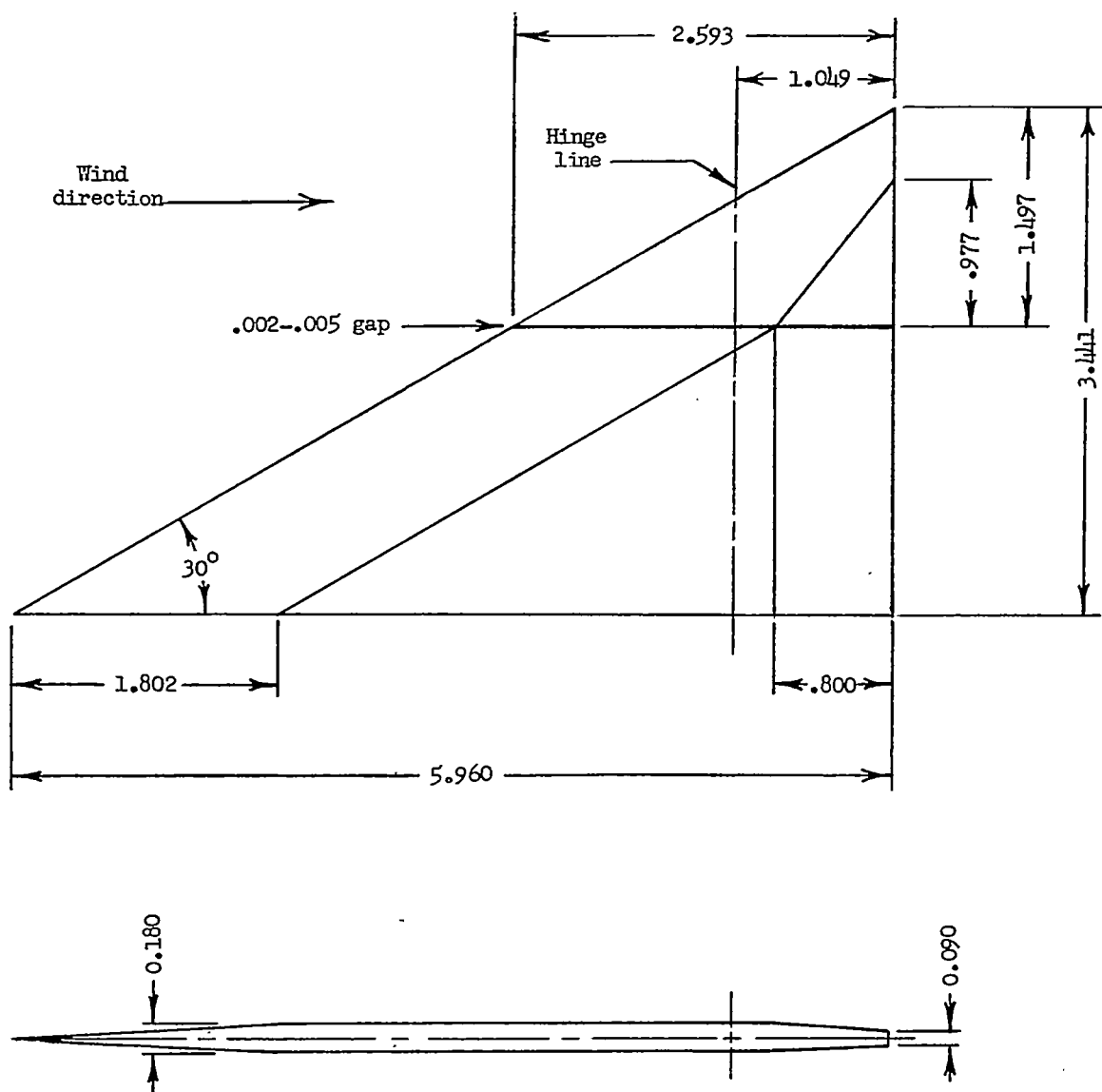
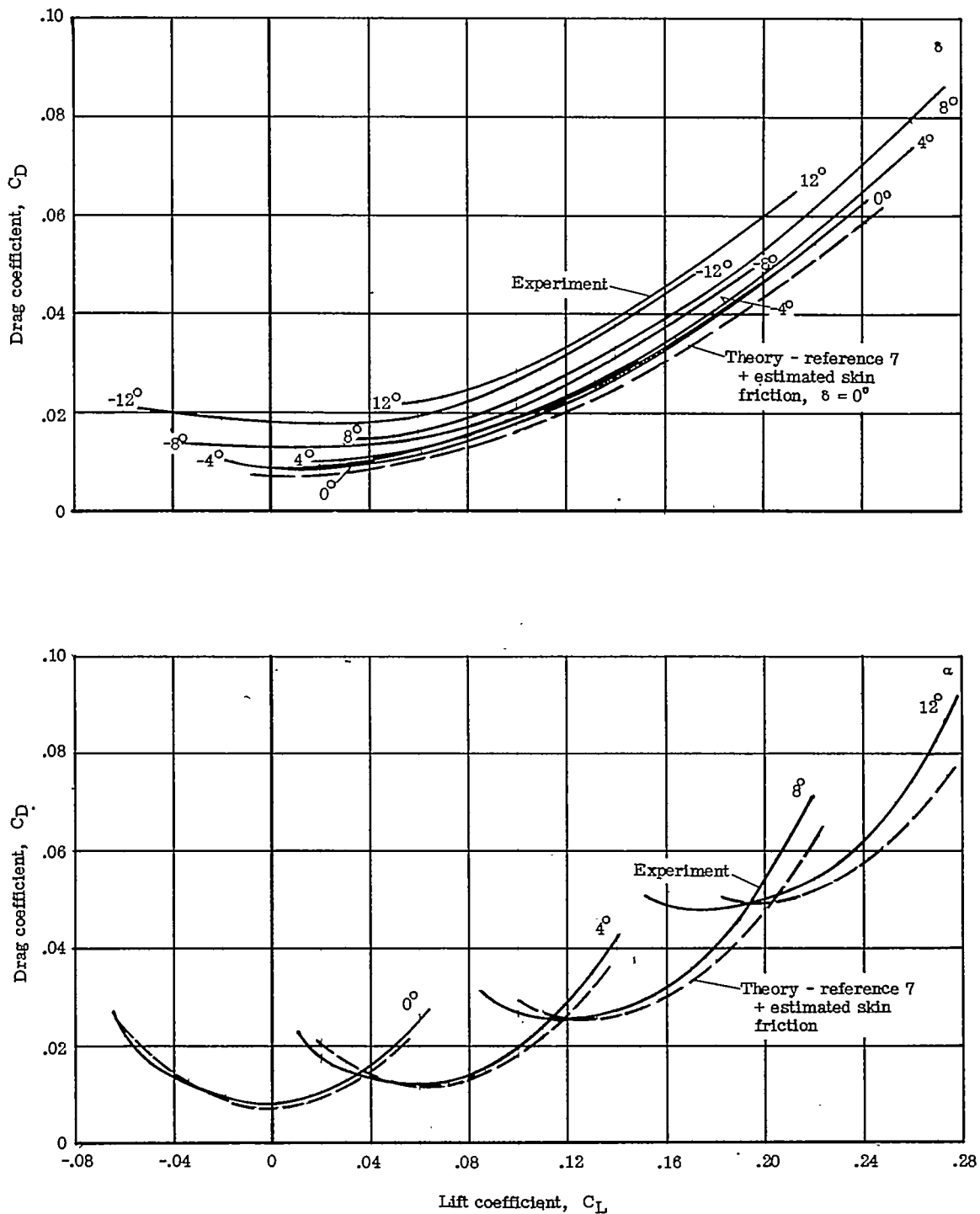
~~CONFIDENTIAL~~

Figure 3.- Diagram of test configuration. All dimensions are in inches.

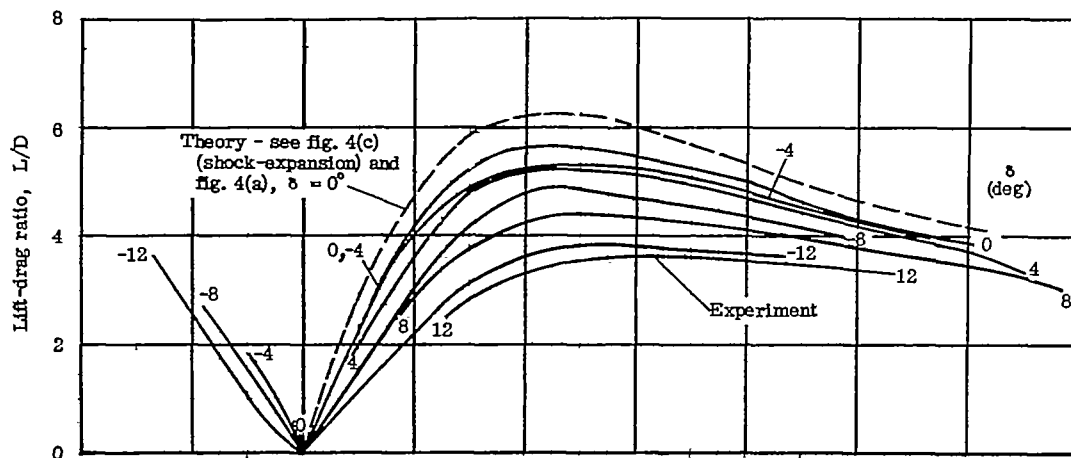
~~CONFIDENTIAL~~



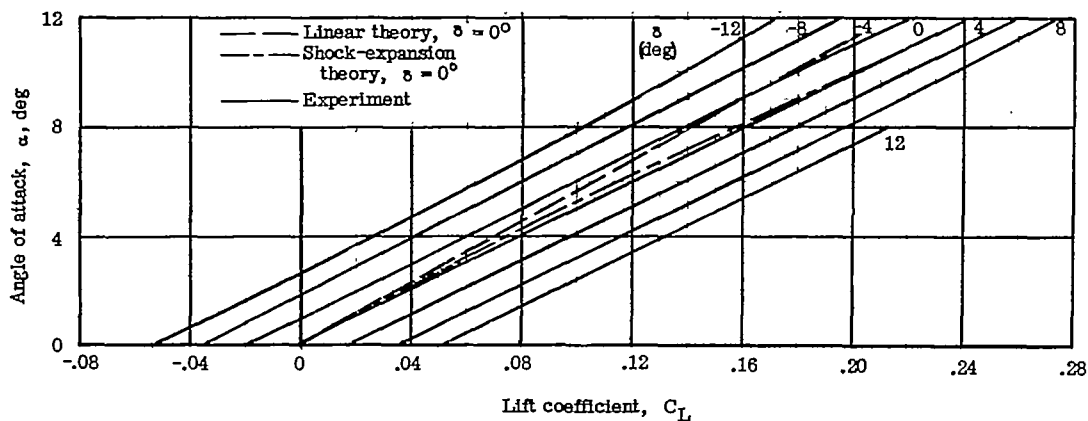
(a) Drag coefficient.

Figure 4.- Variation of aerodynamic characteristics with lift coefficient of a  $60^\circ$  delta wing having a half-delta tip control at  $M = 4.04$  and  $R = 5.8 \times 10^6$ .

CONFIDENTIAL



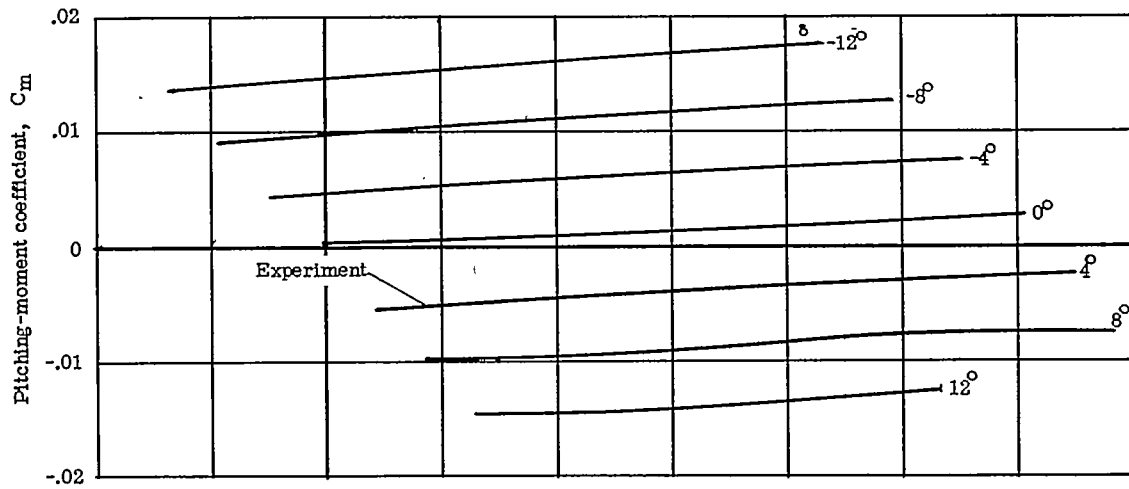
(b) Lift-drag ratio.



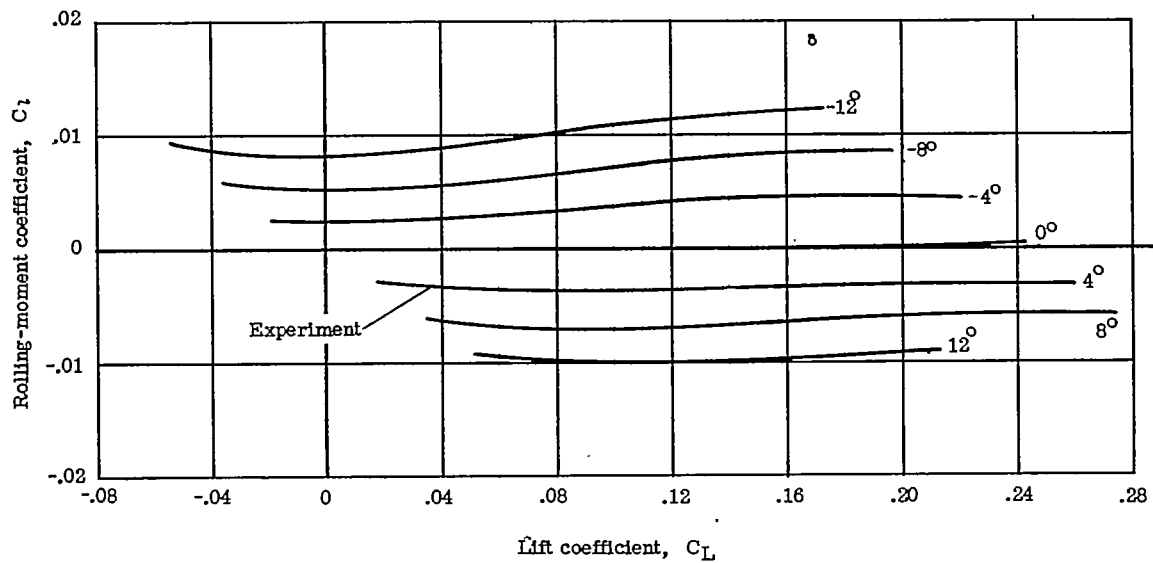
(c) Angle of attack.

Figure 4.- Continued.

CONFIDENTIAL



(d) Pitching-moment coefficient.



(e) Rolling-moment coefficient.

Figure 4.- Concluded.

CONFIDENTIAL

~~CONFIDENTIAL~~

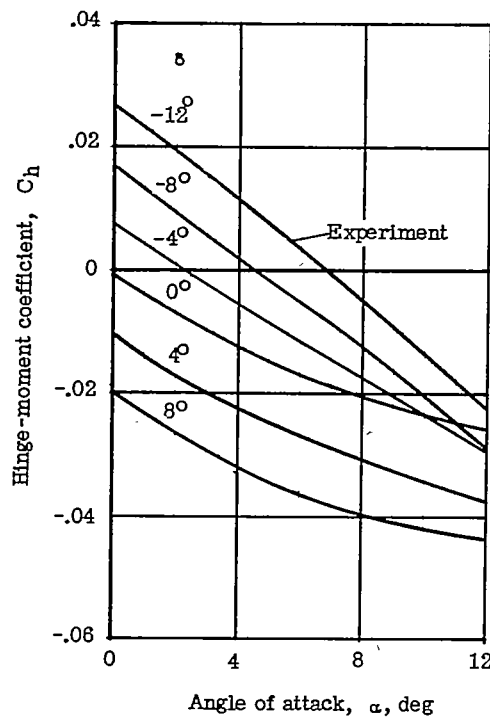
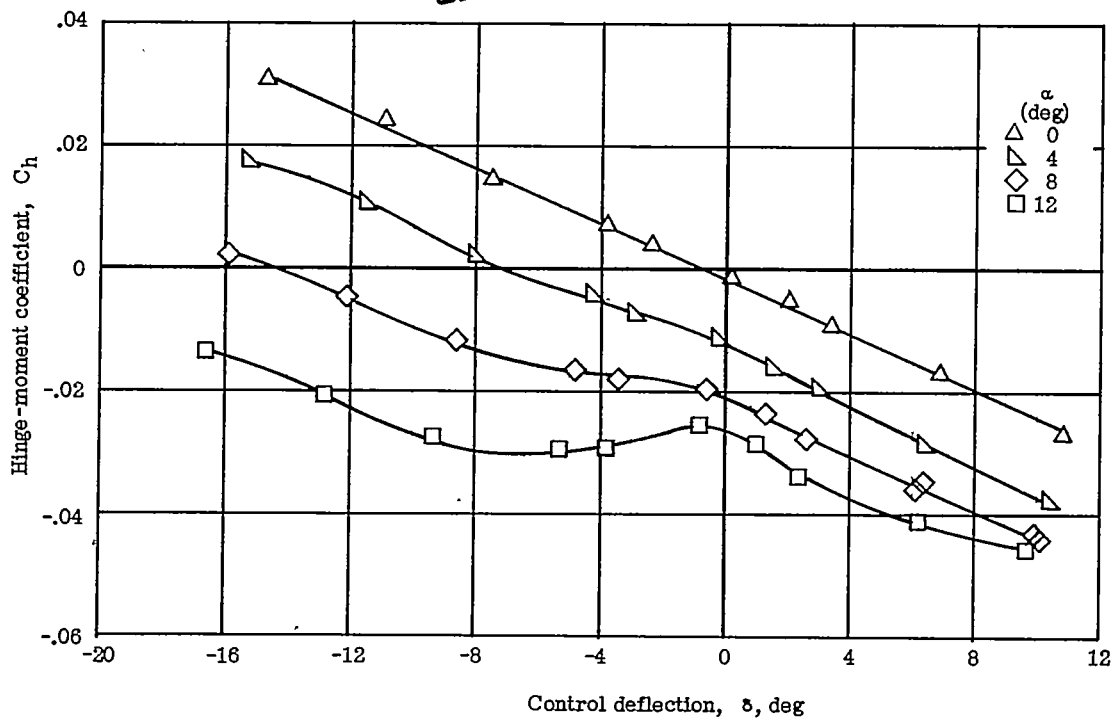
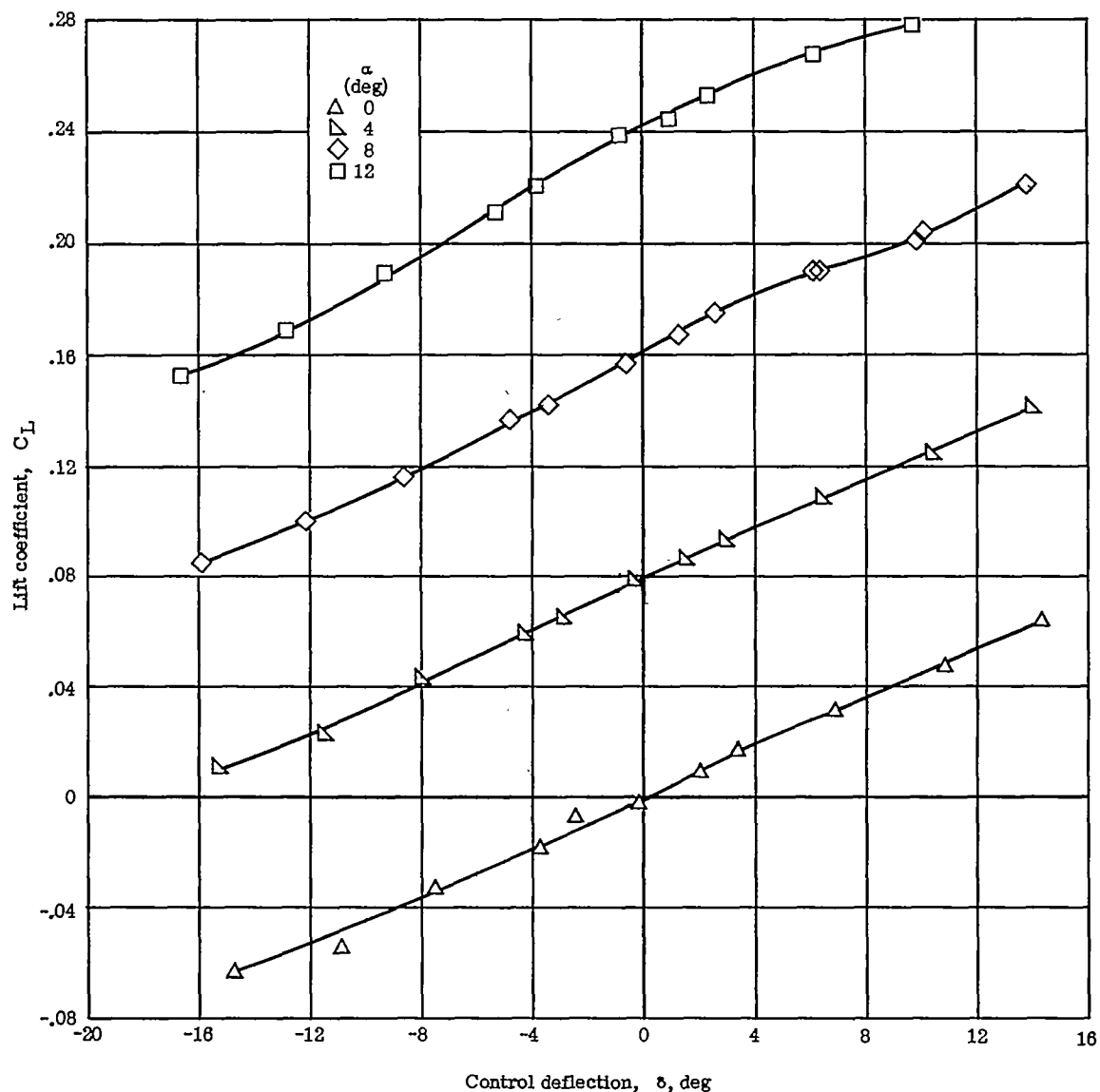


Figure 5.- Control hinge-moment characteristics of a half-delta tip control on a  $60^\circ$  delta wing at  $M = 4.04$  and  $R = 5.8 \times 10^6$ .

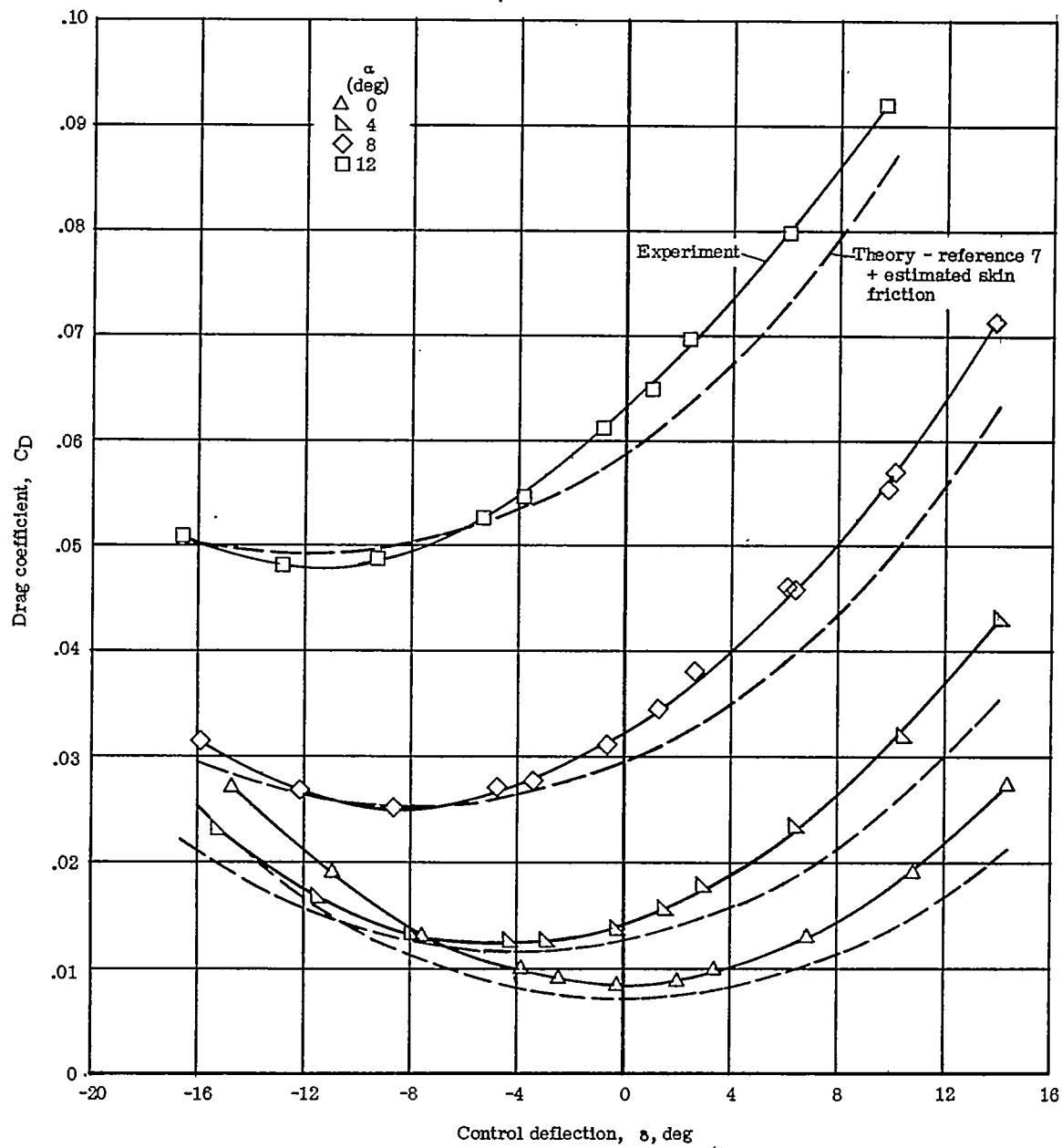
~~CONFIDENTIAL~~

~~CONFIDENTIAL~~

(a) Lift coefficient.

Figure 6.- Variation of aerodynamic characteristics with control deflection of a  $60^\circ$  delta wing having a half-delta tip control at various angles of attack at  $M = 4.04$  and  $R = 5.8 \times 10^6$ .

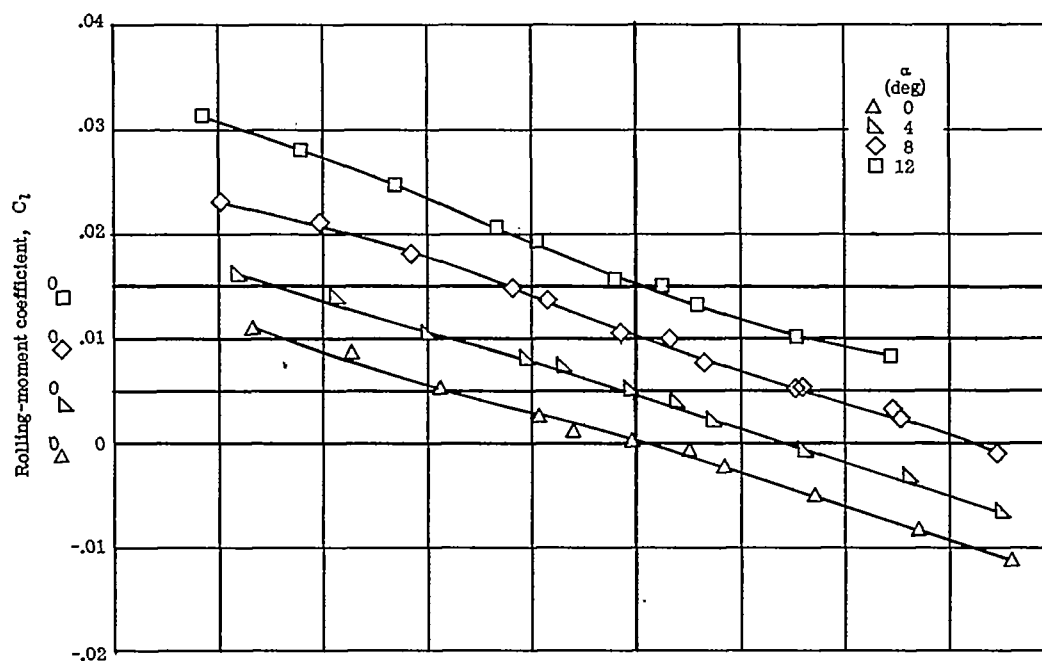
~~CONFIDENTIAL~~



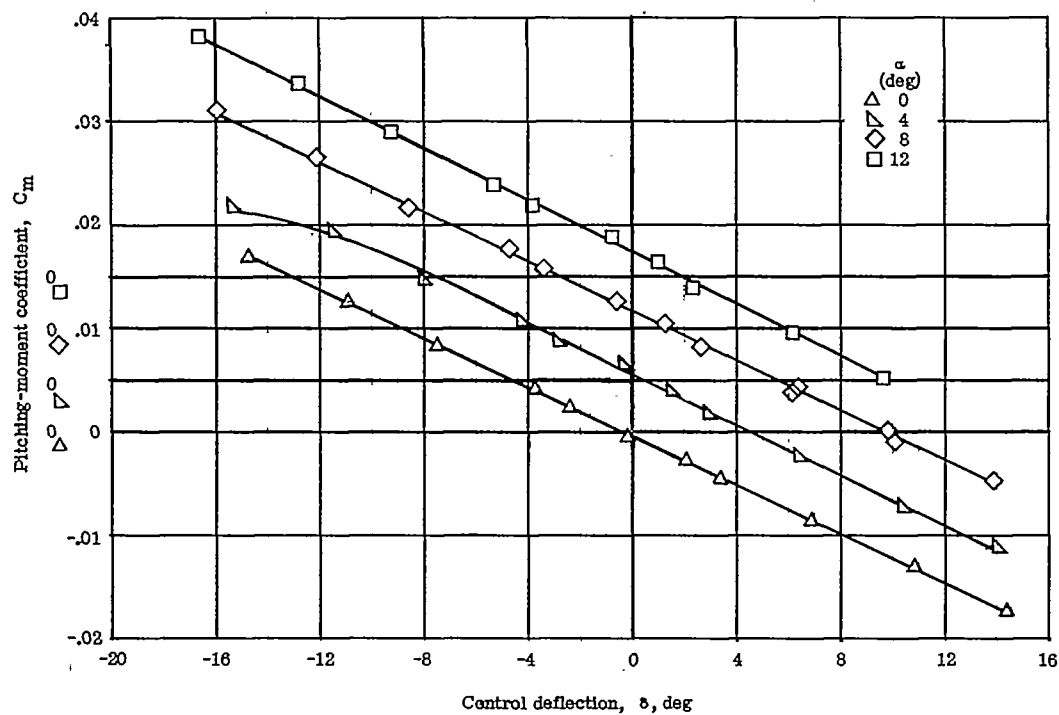
(b) Drag coefficient.

Figure 6.- Continued.

~~CONFIDENTIAL~~



(c) Rolling-moment coefficient.

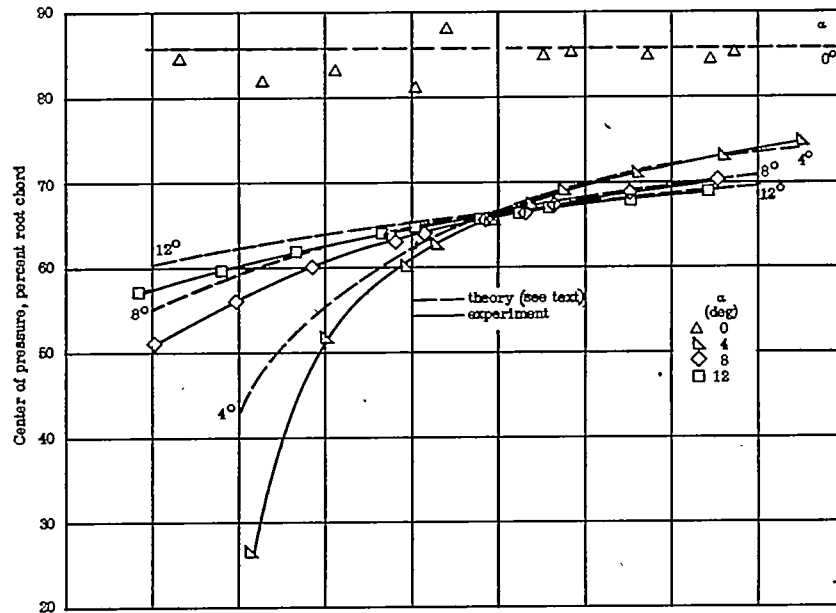


(d) Pitching-moment coefficient.

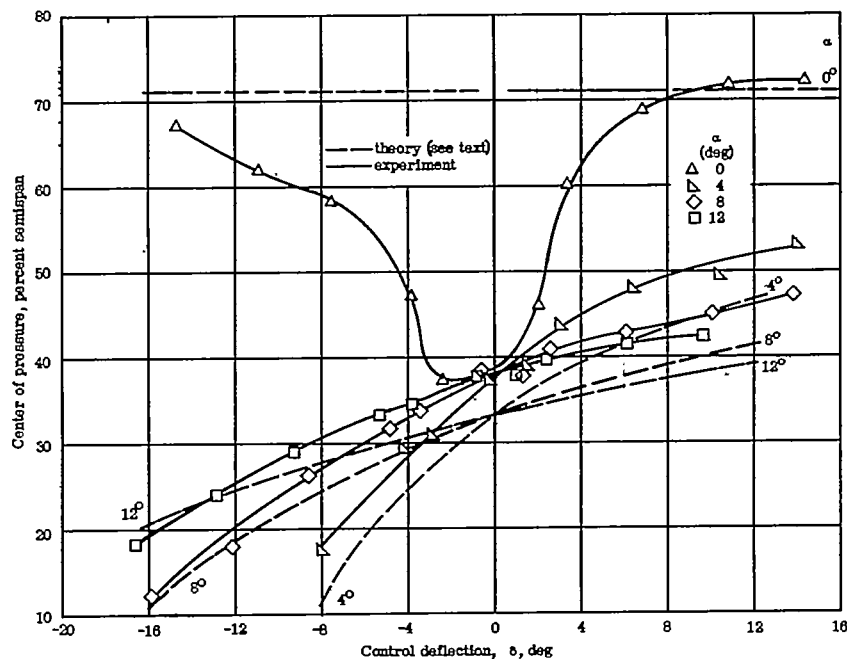
Figure 6.- Concluded.

A. J. G. 1955





(a) Chordwise center of pressure.



(b) Spanwise center of pressure.

Figure 7.- Variation of center-of-pressure locations with control deflection of a  $60^\circ$  delta wing having a half-delta tip control at various angles of attack at  $M = 4.04$  and  $R = 5.8 \times 10^6$ .

CONFIDENTIAL

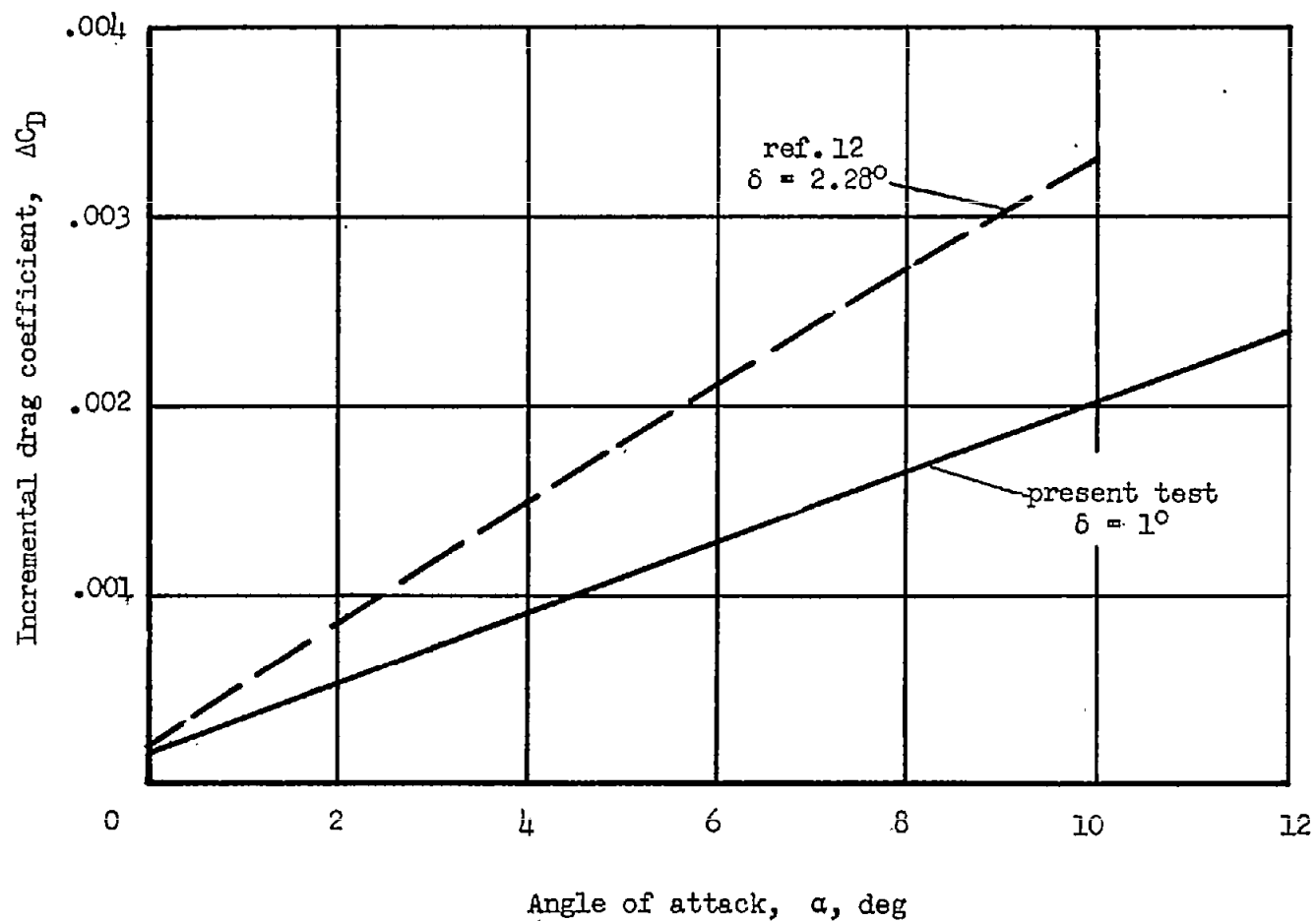


Figure 8.- Comparison of incremental drag coefficients of a half-delta tip control and a full-span trailing-edge rectangular flap-type control at control deflections producing the same wing-tip helix angle.  $M = 4.04$ .

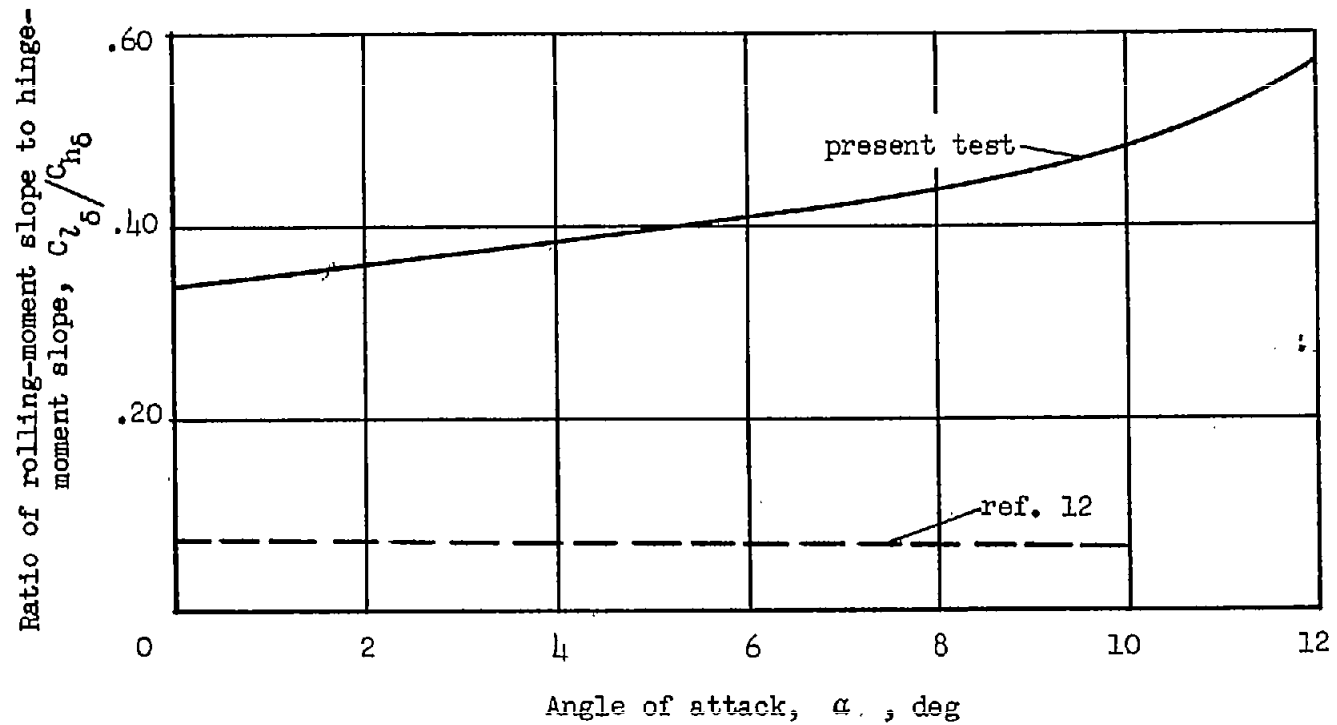


Figure 9.- Comparison of ratios of rolling-moment slope to hinge-moment slope of a half-delta tip control and a full-span rectangular trailing-edge flap-type control at  $M = 4.04$ .